UNIVERSITÉ DE GENÈVE
FACULTÉ DES SCIENCES

Bachelor Research Project

Arabidopsis Extra-Large G Proteins (XLGs) in phosphate homeostasis

Presented by

IRENE SABATER ROYO

Supervisors:

Martina Ried
Michael Hothorn

Department of Botany and Plant Biology,
Faculty of Sciences, University of Geneva.

INDEX

Page

1. Abstract …… 1
2. Introduction ……..2
3. Aims of this work and experimental approach……. 5
4. Material and methods ……..…… 5
5. Results ……..……9
   - 5.1 Golden Gate cloning ……..……9
   - 5.2 *Xlg* mutants are not impaired in seed germination under different light and temperature conditions ……...10
   - 5.3 *Xlg* mutants have a reduced shoot phosphate content ..……11
   - 5.4 Primary root length of *xlg* mutants is reduced under Pi starvation conditions ……12
   - 5.5 Transcript levels of phosphate starvation induced genes are higher in *xlg* mutants ……..……14
   - 5.6 Yeast two-hybrid assay ……15
     - 5.6.1 Fine-mapping of the minimal XLG fragment required for SPX interaction in yeast …..…….....16
     - 5.6.2 Interaction of XLG and SPX is dependent on IPs in yeast 17
   - 5.7 XLG3 is hypersensitive to brassinazole treatment …….……..19
6. Discussion and conclusion ..……..21
7. References…….. 23

Appendix ……. I - VII

1. ABSTRACT

Phosphorus, which is taken up as inorganic phosphate (Pi), is one of the most limiting nutrients for plants. To maintain Pi homeostasis, many proteins (e.g. SPX domain proteins) are involved in signalling pathways to mediate different plant responses.

In addition to the canonical heterotrimeric G proteins, the *Arabidopsis* genome encodes three Gα-like proteins, named Extra-Large G proteins: XLG1, XLG2, and XLG3. This project study the role of XLGs in Pi homeostasis in *Arabidopsis thaliana*. Analysis of the shoot Pi content showed a decreased accumulation in *xlg1*-2 and *xlg3-2* single mutants, which is more notable in the *xlg1-2 xlg3-2* double mutant. Under Pi starvation, the *xlg1-2 xlg3-2* double mutant developed longer primary roots compared to wild-type plants, while the single *xlg* mutants were not significant different. Furthermore, all tested *xlg* single and double mutants showed a tendency toward increased transcript levels of phosphate starvation induced genes compared to the wild-type. Additionally, yeast two-hybrid assays showed an interaction between SPX proteins and XLG1 and XLG3. AtSPX1, a phosphate-dependent inhibitor of the MYB-type transcription factor Phosphate Starvation Response 1 (PHR1), interacts with both AtXLG1 and AtXLG3. However, AtSPX-MFS1, a vacuolar transporter that mediates phosphate storage, only interacts with AtXLG3. These results suggest that XLGs proteins may play a role in Pi homeostasis together with SPX proteins.

To test for brassinosteroid related phenotypes, plants were treated with the brassinosteroid biosynthesis inhibitor brassinazole (BRZ). The *xlg3-2* mutant showed a decreased in hypocotyl length compared to wild-type, while the *xlg1-2* and *spx1-1* mutants did not. The *xlg1-2 xlg3-2* double mutant showed the same tendency as the *xlg3-2*, suggesting that the phenotype is caused by the *XLG3* mutation.

Taken together, these results suggest that XLGs proteins may be involved in different signaling pathways. Nevertheless, little is known about these signalling proteins, and further studies are needed to define how they work.

2. INTRODUCTION

Phosphate homeostasis and SPX domain-containing proteins.

It is well established that the availability of nutrients in soil influences plant growth and development (López-Buicio et al., 2003). Inorganic phosphate (Pi), the main source of phosphorus for plants, is present in a low bioavailability in soil, mainly because it is often bound to organic and inorganic compounds creating insoluble complexes (Marschner et al., 1995). To cope with these conditions, plants have developed mechanisms to facilitate Pi acquisition.

At the developmental level, *Arabidopsis thaliana* profoundly adapts its root system architecture (RSA) to overcome Pi deficiency and promote topsoil foraging via the inhibition of primary root growth, an increase in lateral root formation and the development of root hairs (Peret et al., 2011). Additionally, roots secrete organic acids or phosphatases (Poirier and Bucher, 2002), and engage in plant root symbioses with mycorrhizae fungi in order to improve the solubility and acquisition of Pi (Ezawa and Saito, 2018).

At the genetic level, hundreds of genes are differentially upregulated in response to Pi deficiencies and are thus named phosphate starvation induced (PSI) genes. The MYB-type transcription factor Phosphate Starvation Response 1 (PHR1) and its homologue PHL1 (PHR1-like 1) control the expression of PSI genes responsible for the various adaptations to Pi deficiency (Rubio et al., 2001). Since *PHR1* mRNA levels are unaltered under Pi starvation conditions, it remains an open question how PHR1 activity is regulated by Pi deficiency (Jung et al., 2017).

Hydrophilic SPX domains are found at the N-termini of various proteins, particularly in those involved in signal transduction. Depending on the presence of additional domains, plant SPX proteins can be divided into four groups. The first one corresponds to proteins that only contain the SPX domain, while groups 2 to 4 represent proteins that harbor at the C-terminus an EXS domain, a MFS domain or a RING domain, respectively. In *A. thaliana,* group 1 of SPX proteins consists of four proteins of about 280 amino acids, named AtSPX1–AtSPX4 (Secco et al., 2012).

In *A. thaliana,* all four stand-alone *SPX* genes are implicated in Pi starvation. While low Pi availability induces expression of *AtSPX1* and *AtSPX3*, *AtSPX2* is only weakly induced and *AtSPX4* is suppressed (Duan et al., 2008). It is assumed that both, *AtSPX1* and *AtSPX3*, play positive roles in plant adaptation to Pi starvation, and that *AtSPX3* may have a negative feedback regulatory role in *AtSPX1* response to Pi starvation (Duan et al., 2008).

PHR1 induces the expression of PSI genes under Pi starvation conditions. In the presence of Pi, SPX1 influence the PHR1–DNA-binding, preventing PSI genes expression (Puga et al., 2014 and Qi WJ. et al., 2017). Recently, inositol polyphosphates (InsPs) have been implicated in Pi deficiency signalling mediated by PHR1. InsPs concentration changes in response to Pi availability, and they can be further phosphorylated to inositol pyrophosphates (PP-InsPs). The new hypothesis support that InsPs signal the cellular Pi status and promote the specific interaction of SPX proteins with target transcription factors, such as PHR1 (Wild et al., 2016).

Heterotrimeric G protein signalling in the plant kingdom

Heterotrimeric G proteins, comprising Gα, Gβ, and Gγ subunits, perceive extracellular stimuli through cell surface receptors and transduce these signals into intracellular physiological responses. The *Arabidopsis* genome encodes one canonical Gα (*GPA1*), one Gβ (*AGB1*), and two canonical Gγ subunits (*AGG1*, *AGG2*) (Urano et al., 2013). In addition to *GPA1*, which is involved in a wide range of developmental processes (Ullah et al., 2001), the *Arabidopsis* genome also encodes three unique Gα-like proteins, named Extra-Large G proteins: XLG1, XLG2, and XLG3 (Lee and Assmann, 1999; Ding et al., 2008).

XLGs are composed of a C-terminal Gα-like domain and a N-terminal extension containing a nuclear localization signal and a cysteine-rich region (Lee and Assmann, 1999). Gβγ dimers directly interact with XLGs, suggesting that XLG proteins could originate from a canonical Gα subunit and retained prototypical interaction with Gβγ dimers (Maruta et al., 2015). However, differences between XLGs and Gα subunits have been characterized. Regarding the catalytic activity, XLG proteins bind and hydrolyse guanine nucleotides using calcium as cofactor, but not magnesium like canonical Gα proteins. Additionally, the GTPase activity was less than that of GPA1 in the presence magnesium (Heo et al., 2012).

Arabidopsis *xlg1-xlg2-xlg3* triple mutants grown in dark showed an increased primary root length compared to wild-type plants, but this phenotype was not observed in dark-grown *xlg* single mutants. Since the root cell size and morphology of the *xlg* triple mutant is highly similar to that of wild-type roots, XLGs may regulate cell proliferation. Dark-grown roots of the *xlg* triple mutants also showed altered sensitivity to sugars and ABA hyposensitivity, whereas seed germination in *xlg* triple mutants was hypersensitive to osmotic stress and ABA (Ding 2008). XLG2 further plays a role in disease resistance (Zhu et al., 2009) and flowering (Heo et al,. 2012).

Similar to AGB1, XLG3 is involved in the regulation of root responses. When seeds were germinated in the presence of an ethylene precursor (ACC), wild-type seedlings showed shorter roots, higher hypocotyls thickness and an enhanced hook angle. These responses were stronger in both *agb1* and *xlg3* mutants, indicating hypersensitivity to ethylene (Pandey et al., 2008).

Golden Gate Cloning (Binder et al., 2014)

For the analysis of protein and gene functions, transgenic plants carrying synthetic DNA sequences are indispensable tools. The Golden Gate (GG) cloning permits the assembly of DNA fragments in a pre-defined order for the construction of binary plasmids for transgene expression. With the GG toolkit you can create a library of elements to easily assemble different constructs, such as promoters, protein tags and genes of interest (GOI). The system is based on type IIS restriction enzymes (e.g. BsaI, BpiI), which generate a 4 bases overhang upon cleavage, and multi-part assembly is achieved by using a cut-ligation reaction. By designing type IIS sites at their flanking 5' and 3' ends, overhangs that anneal in desired combinations can be created, enabling the unidirectional assembly of multiple DNA fragments.

A typical construct is assembled in multiple levels. Functional modules (Level I, LI; e.g. promoter, gene) are combined into an expression cassette (Level II, LII; e.g. promoter:tag:GOI:terminator). Then, LII constructs can be assembled into higher-order constructs containing multiple genes (Level III, IV, etc). Each LII construct is assembled from up to six LI modules containing different elements: promoters, N-terminal tag, GOI, C-terminal tag, terminator and resistance marker. The LI modules are combined with a LII vector backbone by BsaI cut-ligation. Subsequently up to five LII synthetic genes can then be assembled into a single LIII vector backbone by BpiI cut-ligation. For higher order assemblies, the LII and LIII backbones are reused in successive BsaI and BpiI cut-ligations. For the convenient selection, each vector backbone contains an antibiotic resistance marker different from the previous level.

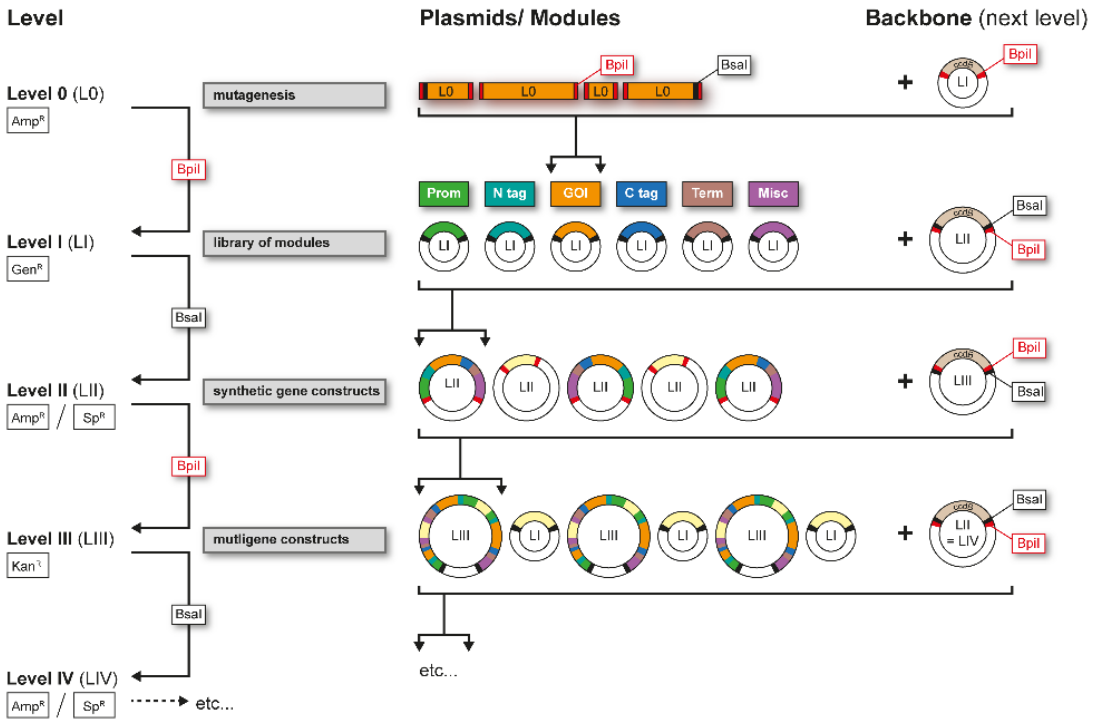

Figure 1. Overview of multi-level construct assembly (Figure taken from Binder et al., 2014).

3. AIMS OF THIS WORK AND EXPERIMENTAL APPROACHES

Since the first plant XLG was described (Lee and Assmann, 1996), only a few studies focused on XLGs. The general role for these proteins centers on stress responses, but downstream targets of the molecular mechanisms are rarely known. The aim of this research project is to study whether XLGs play a role in Pi homeostasis signaling in *A. thaliana*. Additionally, the putative interplay between SPX domain proteins and XLG proteins will be investigated.

For these purposes, phenotypic analyses *in planta* have been carried out, comparing the behaviour of several *A. thliana xlg* single and double mutants, as well as *spx* mutants. At the plant developmental level, the different assays focus on germination rate, the primary root and the hypocotyl length. Additionally, the Pi total content in was measured, as well as the induction of PSI genes. Furthermore, phenotypic interaction studies between AtSPX and AtXLGs proteins have been performed in *Saccharomyces cerevisiae*. Finally, different AtXLGs and AtSPX proteins were cloned using the Golden Gate toolkit for future expression *in planta*.

4. MATERIAL AND METHODS

Golden Gate Cloning

Type IIS restriction sites were removed by site-directed mutagenesis with Bpi and BsaI overhang primers (Table S1). The resulting PCR fragments were inserted into the *lacZ* gene of the pUC57-Amp vector (L0) by a StuI/SmaI optimized cut-ligation protocol, allowing a blue/white selection of the transformed *Escherichia coli* (strand MACH1). For the cut-ligation reactions, 25-50 ng of vector was combined with insert in a molar ratio of 1:10. For a 20 µl reaction, 0.3 µl of restriction enzyme, 1 µl T4 ligase (NEB) and 2 µl ligase Buffer were added. For SmaI, addition of 2 µl NEB restriction buffer 4 was required. The StuI reaction was incubated for 30-50 cycles, cycling between 37°C for 5 min and 25°C for 5 min, followed by heat inactivation at 50 ºC for 5 min and 80°C for 5 min. For the SmaI reaction, the cycling stage was at a fixed temperature of 25ºC. To optimize the reactions, 0.3 µl of fresh enzyme was added together with 0.3 µl of antarctic phosphatase (NEB) and 2 µl of phosphatase reaction buffer. Samples were incubated for another 1 h 37°C for StuI or 25°C for SmaI, and then heat inactivated at 60°C for 20 min. 5 µl of the reaction was transformed into *E. coli* by heat shock and plated on LB plates containing the appropriate antibiotic, supplemented with 50 µg/ml X-Gal and 100 µM IPTG. Colony PCR from white colonies was performed to confirm the right size of the insert. Afterwards, colonies were transferred to liquid culture supplemented with antibiotic and plasmids were purified (MiniPrep kit, Promega) and validated by sequencing.

Plant Material

All *A. thaliana* mutants and the wild-type described in the manuscript were of Col-0 ecotype. Seeds were obtained from "The Nottingham Arabidopsis Stock Centre" – NASC (Scholl et al., 2000). The double mutants *spx1-1 spx2-1* and *xlg1-2 xlg3-2* were obtained by crossing the

respective single mutants. T-DNA insertions in *XLGs*, *SPX*, and *PHR* were verified by PCR analysis using a T-DNA left-border primer (LB1.3) and gene-specific primers (Table S2).

Plate Assays, Seed sterilization and plant growth

A. thaliana seeds were either surface sterilized by incubation for 5 min in a sterilization solution (70 % ethanol, 0.1 % Triton X-100), followed by incubation for 5 min in 2 % bleach and four washing steps with sterile water, or with chlorine gas in a desiccator jar containing a beaker with 50ml bleach and 5ml HCl 37% for 3-4 hours. After 1 hour drying in a sterile bench, 1 ml of distilled water was added. Seeds were stratified at 4 ºC for 2 days, plated and transferred to long-day growth chamber conditions (16 h light/8 h dark cycle, 20 ºC). After one week, seedlings were transferred to soil and grown in a walk-in growth chamber.

Plate assays were performed on 100 mm square plates with standard 0.5 % MS medium containing 0.8 % agar and supplemented with 0 % or 1 % sucrose (MS –Suc; MS +Suc).

Germination assay

Seeds were surface sterilized and directly plated on MS +Suc. 150 seeds of each genotype were analyzed for each condition. Plates were exposed to different treatments (Table 1). The percentages of germination were measured 5 days after seeds were plated.

No Cold/Light	Plates were put directly in a growth room (22ºC, long day condition).
No Cold/Dark	Plates were placed in the dark in a growth room.
Cold/Light	Plates were wrapped in foil and place at 4ºC for 3 days. After the cold treatment, the plates were unwrapped and placed in a growth room.
Cold/Dark	Plates were wrapped in foil and place at 4ºC for 3 days. After the cold treatment, plates were placed in the dark in a growth room.

Table 1. Treatments followed for the germination assay.

Pi extraction

Fresh shoots were harvest (40-180 mg), placed in 1.5 mL eppendorf tubes containing 1 mL desalted water and kept at -20 ºC. For Pi extraction, samples were incubated in a thermo mixer for 1 h at 85 ºC and 1400 rpm. Subsequently, samples were frozen at -80 ºC for 30-45 min and incubated again for 1 h at 85 ºC and 1400 rpm. After the second incubation step, samples were keep at 4 ºC for 45 min.

20 µL of each extract were pipetted into a 96-well plate. Standard Pi solutions (1 mM, 0.5 mM, 0.2 mM, and 0.1 mM NaPi) were used to generate a standard curve. 100 µL of master mix (6.6 mM ammonium molybdate tetra hydrate solution, 4.4 mM 10% ascorbic acid) was added into each well, and the plate was incubating 1 h at 37ºC. The absorbance at 820 nm was measured using a Multi-Mode Microplate Reader (Synergy 2). For each biological replicate, two technical replicates have been analyzed. Experiment was performed 2 times independently.

Hypocotyl elongation

Arabidopsis seeds were surface-sterilized. 100 mm square plates were prepared with 50 mL of 0.5 % MS medium with 1 % sucrose and 0,8 % agar, pH was adjusted to 5.7. The plates MS – Suc medium was either supplemented with 1 µM brassinazole (BRZ; in DMSO) or with 0.01 % DMSO as control. On each plate, seeds were sown in two rows. Each row contained 4 blocks of 10 to 13 seeds of one genotype each (Figure 2). For each genotype, 200-250 seeds were plated.

The plates were sealed with aluminium foil to keep them dark and stored vertically at 4 °C for 2 days. Next, seeds were exposed to light for 3 h to stimulate seed germination and subsequently incubated at 22 ºC for 5 days is the dark. Plates were scanned on a regular flatbed scanner and hypocotyls were measured using FIJI (Schindelin J. et al., 2012).

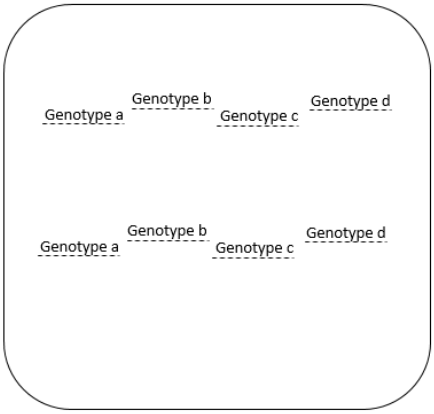

Figure 2. Schema of distribution of seeds on the plates.

The hypocotyl lengths were quantified using the package multcomp (Hothorn et al., 2008). The data was analyzed by a mixed effects model for the ratio of the mutant lines versus wild type (WT). The ratio of the untreated (C) and treated seedlings (BRZ) was calculated for WT and each mutant line. The ratio of this ratio for WT divided by a given mutant line ratio results in the ratio of ratios.

Root system architecture

Seeds were plated on MS +Suc plates containing either 1 mM or 0.1 mM phosphate (normal P and low P, respectively). 40 seeds were plated per each genotype and phosphate condition. Plates were scanned after 6 and 11 days (same parameters as hypocotyl assay) and the primary root length was measured using NeuroFIJI.

RNA extraction, cDNA synthesis and qRT-PCR analysis of PSI genes

Seedlings were grown for 7 days in liquid MS medium containing 0.1 mM phosphate. For each sample, 80-100 mg (4-6 seedlings) plant material was used for RNA extraction with the RNeasy

Plant Mini Kit (QIAGEN) including DNase I treatment (QIAGEN) to remove genomic DNA. First strand cDNA synthesis was performed from 2000 ng total RNA using the SuperScript® II First-Strand Synthesis SuperMix (Invitrogen™) with oligo(dT) primers. qRT-PCR was performed in 10 µL reactions containing SYBR (Applied Byosintems) in a Real-time PCR detection system (Applied Byosistem). PCR program: 2'-50°C; 40x(15''-95°C; 31'-60°C); 15''-95°C, 15''-60°C); melting curve 95°C – 60°C – 95°C. A primer list can be found in the appendix (Table S3). Expression levels of target PSI genes were normalized against the housekeeping gene *ACTIN8* (Lilly et al., 2010). For every genotype, three biological and three technical replicates were analyzed. Seedlings were grown for 7 days.

Yeast strains and media

For all experiments the haploid L40 strain was used (Table S4). Yeast was either grown on YPAD agar plates (20 g/L glucose, 20 g/L bacto-peptone, 10 g/L yeast extract, 40 mg/L adenine hemisulfate, 20 g/L bactoagar) or YPAD liquid medium (20 g/L glucose, 10 g/L yeast extract, 20 g/L bacto-peptone, 40mg/L adenine hemisulfate, 1L ddH_2O). Experiments were performed on synthetic complete medium (6.7 g/L yeast nitrogen base without aminoacids, 20 g/L glucose, 20 g/L bactoagar, 2 g/L aminoacid mix) or on synthetic dropout (SD) medium lacking histidine, tryptophane and leucine.

Yeast transformation

Yeast cells grown on YPAD plates were resuspended in 50 ml YPAD liquid medium. The titer of the yeast culture was determined by pipetting 200 µL of cells into 900 µl of water into a spectrophotometer cuvette and measuring the OD at 600 nm. (2x10^7 cells/ml were used for 10 transformations). Cells were resuspended in LiAc/TE. Transformation was carried out in a 1.5ml eppendorf containing 50 µl of competent cells and a transformation mix (0.5 µg of plasmid A, 0.5 µg of plasmid B, 0.1 µg ssDNA, 345 µl 40%PEG 1xLiAc/TE). Cells were incubated 50 min at 30 ºC and then 30 min at 42 ºC. Then, cells were plated on SD -L -T +H plates to allow growth only the transformed yeast.

Yeast-two hybrid spotting dilution assay.

For the spotting assay co-transformed cells were counted, washed in sterile water. Cells were spotted in 5 times dilution, starting from 100000 cells, onto SD -L-T-H and SD -L-T-H plates supplemented with 3-Amino-1,2,4-triazole (3-AT) to reduce the background due to basal His expression. Plates were incubated at 37 ºC for 6 days and interaction was assessed by activation of the His reporter gene, which was scored by yeast growth.

5. RESULTS

5.1 Golden Gate Cloning

- Level 0

Since internal type IIS restriction would reduce the efficiency of GG-based construct assembly, they were removed by site-directed mutagenesis (see methods).

After purification, plasmids were sequenced to discard mutations or undesired sequences. Following this protocol, L0 constructs were created for the *XLG1*, *XLG3* and *SPX1* synthetic genes (Table S5).

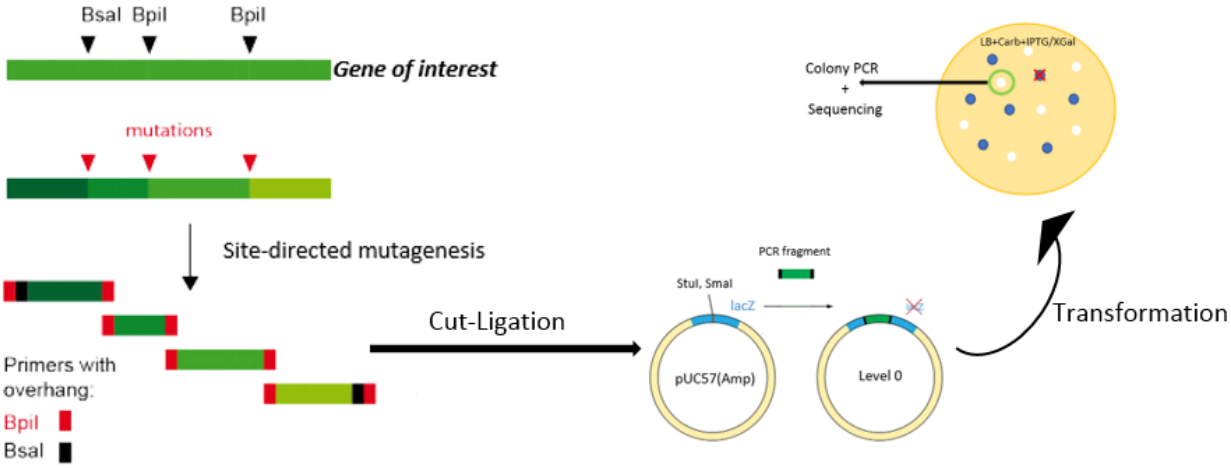

Figure 3. General schema of Level 0 generation. (Figure modified from Binder et al., 2014).

- Level I

The L0 elements for each gene were then assembly in a LI element by a Bpi cut ligation, and they were inserted in the place of a *ccdB* cassette. Thus, only colonies which have lost the *ccdB* cassette, meaning that L0 elements were inserted, are able to growth. After the correct assembly was confirmed by a colony PCR, plasmids were purified. Following these steps, LI modules were created for *XLG1*, *XLG3*, and *SPX1* synthetic genes (Table 2).

As the coding sequence of *SPX3* does not contain any internal type II restriction sites, the target sequence was amplified in a PCR reaction using outer primers containing BsaI sites and an appropriate terminal extension that results in a desired overhang upon BsaI cleavage.

In conclusion, using the GG toolkit, LI modules carrying different elements were generated (Table 2). These LI modules are flanked by BsaI restriction site for further assembly into a LII and subsequently LIII vector backbone suitable for *in planta* gene expression.

Synthetic gene	Module	Antibiotic resistance
SPX1	LI	Gentamicin
SPX3	LI	Gentamicin
XLG3	LI	Gentamicin
XLG1	LI	Gentamicin

Table 2. LI modules carrying *SPX* and *XLG* synthetic genes created using the GG cloning toolkit.

5.2 *Xlg* mutants are not impaired in seed germination under different light and temperature conditions

The first phenotypic assay was performed to study whether *XLGs* or *SPX1* play a role in germination. For this purpose, seeds of the single mutants *xlg1-2, xlg3-2* and *spx1-1* as well as the two *xlg1-2 xlg3-2* double mutant lines DM16 and DM34 were plated and exposed to different treatments (see methods). A *ttm3* single mutant was used as internal control, since germination of this mutant under cold / light conditions has been reported to be reduced to 75% (Laura Lorenzo, unpublished data).

The *ttm3* shows a reduction in germination of about 20% compared to wild-type under both treatments where no cold was applicated. When seeds were exposed to different cold treatments, the percentage of germination was even reduced more (5 times compared to wild-type). However, neither of the tested *xlg* mutants nor the *spx1-1* mutant exhibit a germination rate different to the wild-type under different light and temperatures conditions in a phosphate sufficient medium (Table 3).

	No cold/ Light	Cold/ Light	No Cold/ Dark	Cold/ Dark
Col 0	98,3	99,3	99,3	99,7
xlg1-2	100	99,5	98,5	99,5
xlg3-2	100	96,0	97,5	99,5
DM16	99,7	100	98,5	100
DM34	100	98,5	100	100
spx1-1	100	100	97,9	98,5
ttm3	85,5	27	79,8	24,7

Table 3. Percentage of seeds germinated after been exposed to different treatments.

5.3 *Xlg* mutants have a reduced shoot phosphate content

Having confirmed that the *xlg* mutants show no germination defects under Pi sufficient conditions, the total Pi content of plants was measured. The total Pi content in a plant depends on the uptake of Pi, which is controlled by PSI genes. Thus, to study whether the XLGs proteins impact Pi uptake, total Pi content in shoots of different *xlg* single and double mutants were measured under Pi sufficient conditions.

According to previous results, the *phr1-2 phl1* double mutant has a reduced Pi accumulation compared to wild-type (Bustos et al, 2010), while the *spx1-1 spx2-1* plants showed a significant increase in Pi accumulation (Puga et al., 2014). The single *spx1-1* mutant showed a marginal effect on Pi accumulation (data not shown).

When the Pi content of 17 days old shoots was measured, the two *xlg1-2 xlg3-2* double mutant lines analyzed (DM16 and DM34) showed a significant decrease in Pi accumulation compared to the wild-type. In the case of the *xlg1-2* and *xlg3-2* single mutants, the effect was smaller and similar between both, indicating a functional redundancy between these XLGs proteins (Figure 3). To confirm the significant differences, a Dunnett's post-hoc test was performed, to compare each mutant genotype to the wild-type (Table 4). The data obtained allows us to confirm the hypothesis that there is a relation between the Pi content and the different *XLG* genotypes.

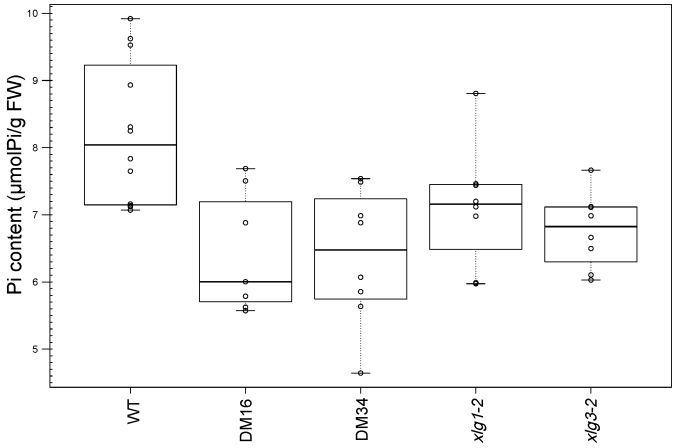

Figure 4. Boxplot showing the Pi levels in wild-type (WT), *xlg1-2* and *xlg3-2* single mutant plants and *xlg1-2xlg3-2* double mutants (DM16 and DM34), all grown in sufficient Pi condition for 17 days.

	Estimate	Std. Error	t value	Pr(>|t|)
DM16 - wt	-1.8280	0.4163	-4.391	< 0.001 ***
DM34 - wt	-1.8242	0.4163	-4.382	< 0.001 ***
xlg1 - wt	-1.0901	0.4163	-2.619	0.04446 *
xlg3 - wt	-1.4390	0.4163	-3.457	0.00496 **

Table 4. Dunnett'st test comparing each single and double *xlg* mutants with wild-type (wt).. Significant codes: 0'***'; 0.001'**'; 0.01'*'.

When the assay was done with plants grown for 3 days more, the phenotype was not as remarkable (Figure S1 and Table S6). This difference could be because at this age, most of the plants have already started to develop the primary shoot. At this stage of development, the plant takes up more water, meaning that the Pi content would be diluted and thus the final concentration altered.

5.4 Primary root length of *xlg* mutants is reduced under Pi starvation conditions

It has been reported that the *xlg2-1 xlg3-1* double mutant and the *xlg1-1 xlg2-1 xlg3-1* triple mutant showed longer primary root as to wild-type plants when they were grown in darkness (Ding et al., 2008). In addition, the RSA of Arabidopsis is influenced by the phosphate availability. Thus, to study if XLG1, XLG3 and SPX play a role in Pi homeostasis, the primary roots of single and double mutants grown under low and high Pi conditions were measured.

The primary root length of 6 days old seedlings grown under low and sufficient Pi conditions (0.1 and 1mM) of each mutant was compared to wild-type. To analyze the root length differences, a Dunnett's test was performed comparing each mutant genotype to the wild-type. Under normal phosphate conditions, all mutant lines show the same tendency as wild-type plants (Figure 5 and Table 5), suggesting that the root structure of these mutant lines are not affected. However, under Pi starvation, both *xlg1-2 xlg3-2* double mutants are significant different from the wild type, as well as the double mutant *phr1-2 phl1*. While both *xlg* double mutants showed an increased in the root length, the *phr1-2 phl1* seedlings have decreased root lengths. These differences are not so clear for the single *xlg* mutants, suggesting that both *XLG1* and *XLG3* are responsible for the phenotype observed in the double mutant lines. The *spx1-1 spx2-1* mutant shows a tendency to form shorter primary roots, but the phenotype in this line is not as remarkable.

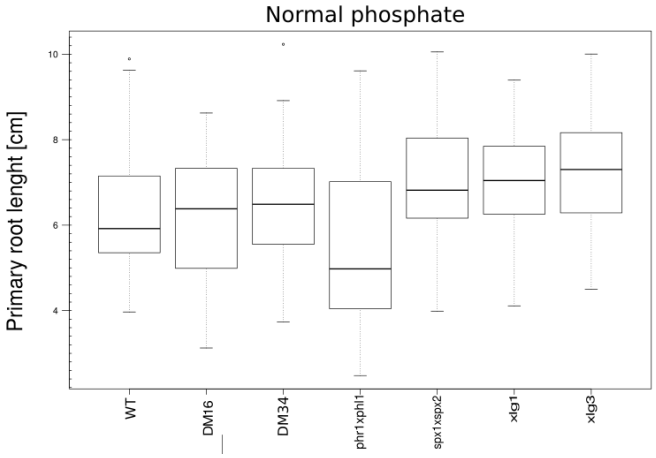

Figure 5. Boxplot showing the primary root lengths in wild-type (WT), *xlg1-2* and *xlg3-2* single mutants, *xlg1-2 xlg3-2* double mutants (DM16 and DM34), *phr1-2 phl1* and *spx1-1 spx2-1* double. Roots were measured 6 days after germination under normal phosphate (1mM) conditions.

	Estimate	Std. Error	t value	Pr(>|t|)
DM16 - WT	0.1270	0.3227	-0.393	0.9977
DM34 - WT	0.2175	0.3397	0.640	0.9714
phr1-2phl1 - WT	-0.7898	0.3827	-2.064	0.1698
spx1-2spx2-1 WT	0.7177	0.3634	1.975	0.2034
xlg1-WT	0.7422	0.3271	2.269	0.1079
xlg3-WT	0.9888	0.3441	2.873	0.0224 *

Table 5. Dunnett'st test comparing each single and double mutants with wild-type (WT) root length under normal phosphate conditions. Significant codes: 0.01 '*'.

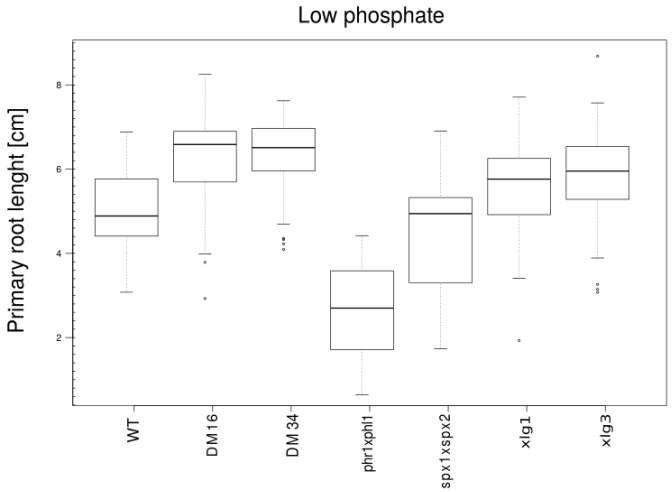

Figure 5. Boxplot showing the primary root lengths in wild-type (WT), *xlg1-2* and *xlg3-2* single mutant plants, *xlg1-2xlg3-2* double mutants (DM16 and DM34), *phr1-2 phl1* and *spx1-1 spx2-1* double. Roots were measured 6 days after germination under phosphate deficient condition.

	Estimate	Std. Error	t value	Pr(>|t|)
DM16 - WT	1.2179	0.2471	4.929	< 0.001 ***
DM34 - WT	1.2983	0.2440	5.322	< 0.001 ***
phr1-2phl1 - WT	-2.3780	0.2926	-8.127	< 0.001 ***
spx1spx2- WT	-0.5508	0.2725	-2.021	0.1796
xlg1-WT	0.5832	0.2460	2.370	0.0826 .
xlg3-WT	0.7714	0.2506	3.078	0.0118 *

Table 5. Dunnett'st test comparing each single and double mutants with wild-type (WT) root length under low phosphate conditions. Significant codes: 0 '***', 0.01 '*' 0.05 '.'

In addition, the root of each seedling was also measured 11 post germination (data not shown) to further analyze the growth of each genotype (difference between the root length of each seedling at day 11 and day 6) under different phosphate conditions.

5.5 Transcript levels of phosphate starvation induced genes are higher in *xlg* mutants

To further study the role of XLG proteins in Pi homeostasis, the expression of PSI genes (*SPX3* and *MGD3*) was analysed via RT-qPCR in the Col-0 wild-type as well as the *xlg1-2*, *xlg3-2*, DM16 and DM34 *(xlg1-2xlg3-2)*, *spx1-1 spx2-1* and *phr1-2 phl1* mutant backgrounds under Pi deficient condition.

In line with previous results, the relative expression of PSI genes was enhanced in the *spx1-1 spx2-1* mutant (Puga et al., 2014; this study), while the *phr1-2 phl* mutant showed a reduced expression of PSI genes compared to the wild-type (Bustos et al. 2010; this study). For the *xlg* mutants, a clear tendency toward increased transcript levels of PSI genes compared to the wild-type was detected. However, due to the considerable high variation of the data, conclusions have to be drawn with caution.

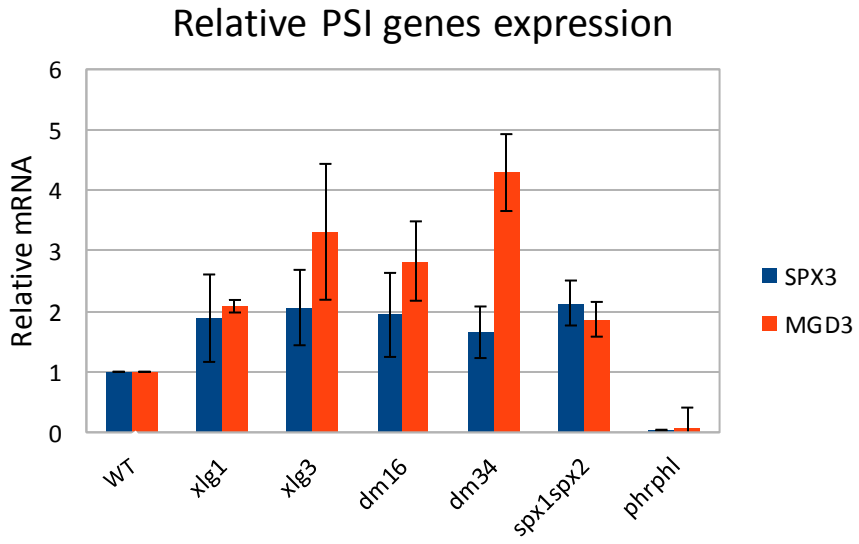

Figure 6. Relative expression of PSI genes in double and single mutants compared to wild-type (WT). Error bars represent the standard deviation.

5.6 Yeast-two hybrid assay

The phenotypic analyses of *xlg* mutants suggest that XLGs may play a role in Pi homeostasis. Thus, an interaction assay between SPXs and XLGs proteins was performed, since maybe these proteins could cooperate in the same phosphate signalling. Previously, a yeast two-hybrid screen identified XLGs as interactors of SPX1 and further interaction studies in yeast showed that both AtXLG1 and AtXLG3 interacted with AtSPX1, while AtSPX-MFS1 only interacted with AtXLG3 (Rebekka Wild, unpublished). The important parts for interaction have been previously mapped down to XLG1mini und XLG3mini (Martina Ried, unpublished), which contain a cysteine rich domain (Figure 7). This assay was carried out to check whether even smaller fragments (AtXLG1sm and AtXLG3sm) still interact with AtSPX1 and AtSPX-MFS1.

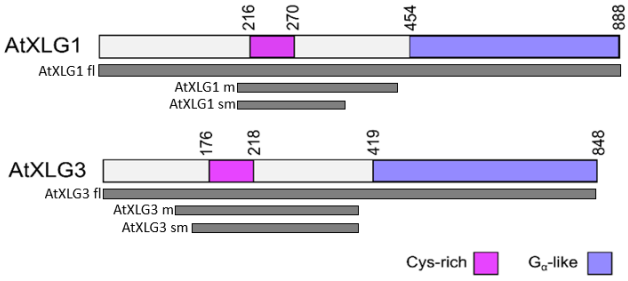

Figure 7. Schema of domains cloned in each construct.

A second aim of this assay was to study whether the presence of PP-InsP can affect the interaction of AtSPX and AtXLG proteins. To check if the interaction is PP-InsP dependent, both proteins of interest were transformed into a L40 ΔVip1 yeast strains (Table S4). Vip1, which catalyzes the production of 1-InsP$_6$ and 1,5-InsP$_6$ from InsP$_6$ and 5-InsP$_6$, respectively (Figure 8, Wild et al., 2016), is no longer active in this ΔVip1 yeast strains.

For both approaches, diploid AtBRI1-AtBKI1 yeasts were used as positive control (Wang X, 2006), and the diploid cells carrying an empty vector pP6 as negative control. Some constructs were already expressed in the wild-type and ΔVip1 strains (Table S4.1). The rest were transformed into L40 strains, either wild-type or ΔVip (Table S4.2).

Construct	Domain	Vector
AtXLG1 fl	1 – 888	pP6
AtXLG1 mini	210 – 430	pP6
AtXLG1 supermini	210 – 410	pP6
AtXLG3 fl	1 – 848	pP6
AtXLG3 mini	130 – 360	pP6
AtXLG3 supermini	160 – 360	pP6
AtBRI1	1 – 1196	p29
AtBKI1	1-337	pP6
AtSPX-MFS1	1 – 240	pP29
AtSPX1	1 – 252	pP29

Table 6. Constructs used for yeast transformation.

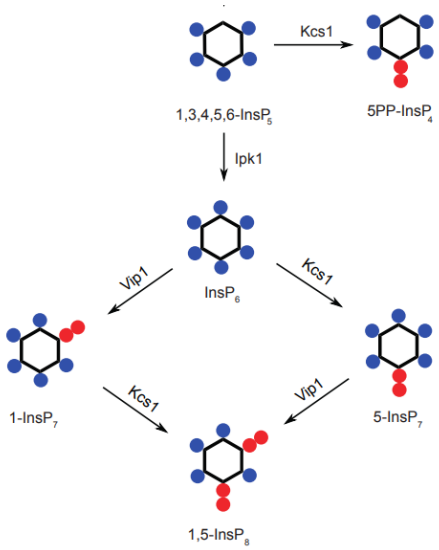

Figure 8. PP-InsP synthesis pathway (Wild et al., 2016).

5.6.1 Fine-mapping of the minimal XLG fragment required for SPX interaction in yeast

According to previous results, AtSPX1 and AtSPX-MFS1 interacts with all mini constructs checked (Martina Ried, unpublished). Additionally, we can see that the AtXLG3sm is still able to interact with both AtSPX1 and AtSPX-MFS1. However, the AtXLG1sm does no longer interact with AtSPX1 (Figures 9 and 10).

These results suggest that in the AtSPX1-XLG1 interaction, the Cys-rich construct is not enough for the successful interaction. Nevertheless, the AtXLG3 seems to require only the Cys-rich domain for its interaction with both AtSPX1 and AtSPX-MFS1.

5.6.2 Interaction of XLG and SPX is dependent on IPs in yeast

Comparing the growth of wild-type and mutant yeasts, we can check whether the interactions are 1-$InsP_6$ or 1,5-$InsP_6$ dependent. Both AtSPX1-XLG1 and AtSPX1-XLG3 interaction look slightly weaker in the ΔVip1 yeasts compared to the wild-type, and the AtSPX-MFS1 interaction is markedly reduced in ΔVip1 yeasts. These results indicate that the interaction between AtSPX1 or AtSPX-MFS1 and AtXLG1 and AtXLG3 are 1-$InsP_6$ or 1,5-$InsP_6$ dependent.

It is important to take in account that maybe the level of protein expression is not the same in the different yeast strains. Therefore, to confirm that the level of yeast growth is proportional to the interaction, it would be necessary to do a protein extraction and quantification via immunoblot.

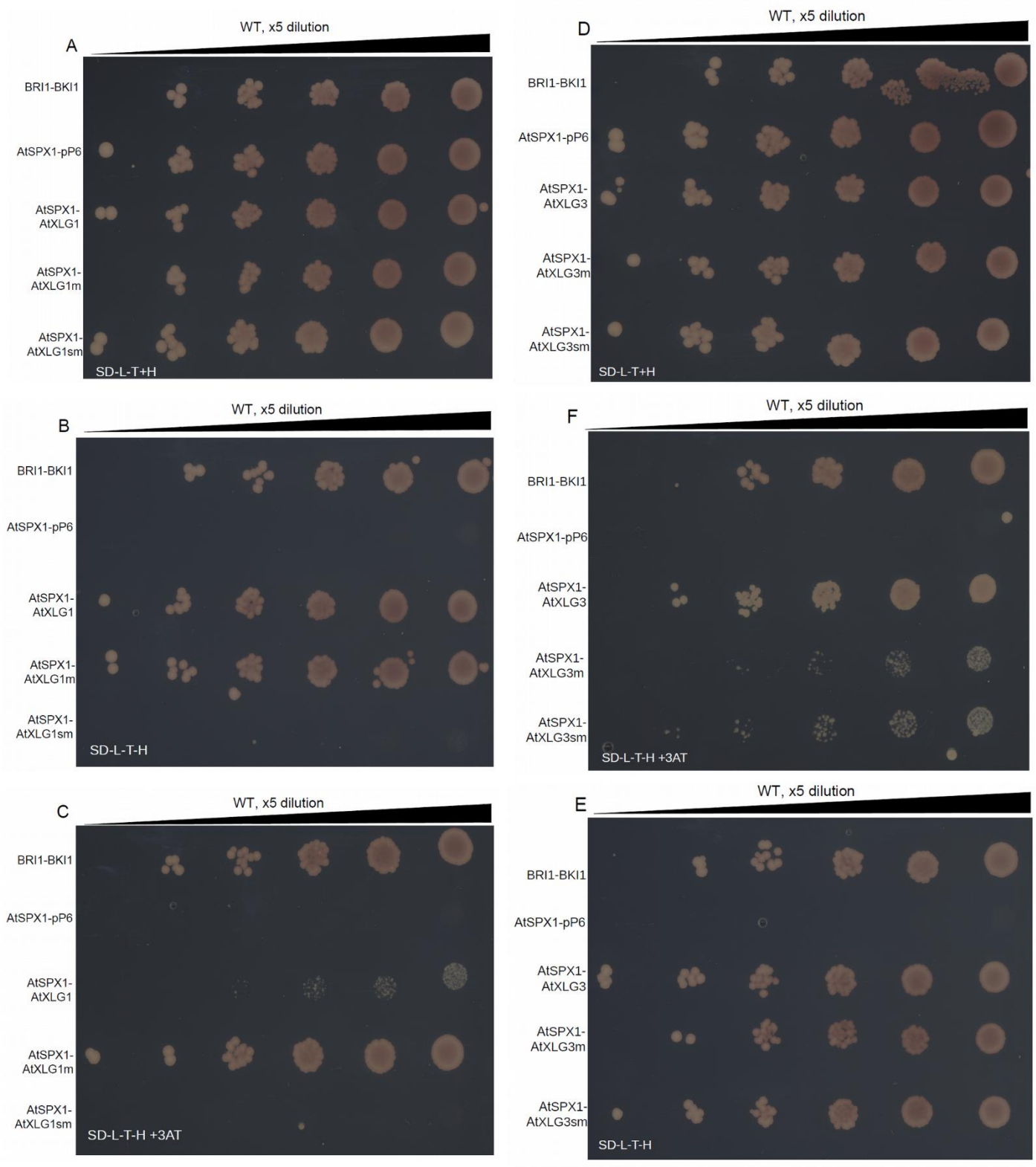

Figure 9. Yeast two hybrid assay. A to C show diploid WT yeast carrying AtSPX1 and different AtXLG1 constructs, plated on SD -L -T +H (A), SD -L -T -H (B) and SD-L-T-H + 3-AT (C). D to F show diploid WT yeast carrying AtSPX1 and different AtXLG3 constructs, plated on the same conditions.

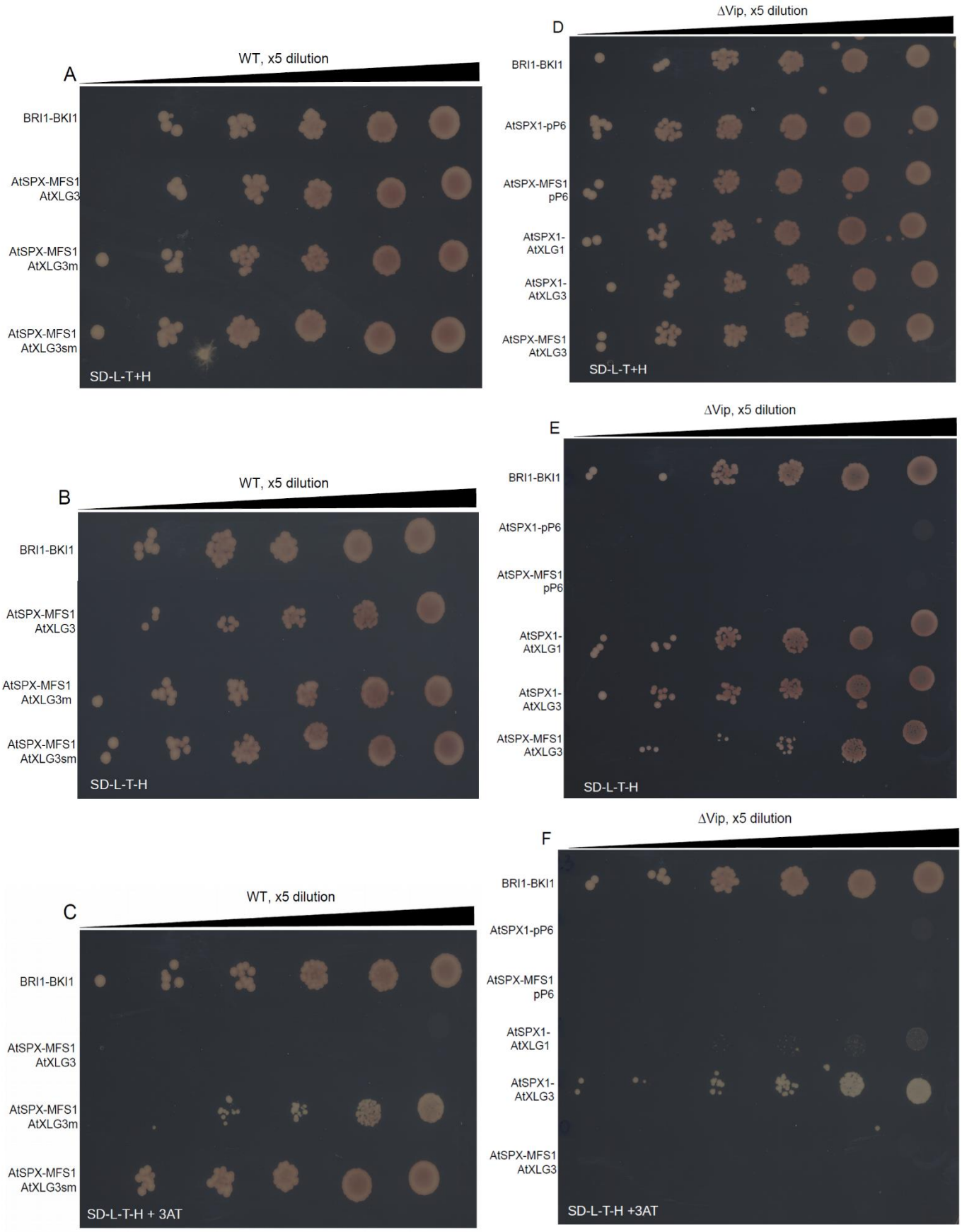

Figure 10. Yeast two hybrid assay. A to C show diploid WT yeast carrying AtSPXmFS1 and different AtXLG1 constructs, plated on SD -L -T +H (A), SD -L -T -H (B) and SD-L-T-H + 3-AT (C). D to F show diploid ΔVip1 yeast carrying AtSPX1 or AtSPXmFS1 and different AtXLG constructs, plated on the same conditions.

5.7 XLG3 is hypersensitive to brassinazole treatment

Brassinosteroids (BR) are steroid plant hormones whose signal is transduced by a receptor kinase-mediated signal transduction pathway. There are thousands of BR target genes, linking BR signaling to numerous cellular processes that regulate plant growth, development and metabolism (Zhu et al., 2013). Brassinazole (BRZ) is a specific brassinosteroid biosynthesis inhibitor (Asami at al., 2000) used to study BR functions, since it causes changes in plants almost identical to those found in BR-deficient mutants.

This assay was carried out to study whether XLGs are involve in brassinoesteroid (BR) signaling. For this purpose, the hypocotyl length of different mutant and wild-type seedlings were measured and analyzed either in the presence BRZ or under unchallenged conditions. The genotypes analyzed were *xlg1-2*, *xlg3-2*, *spx1-1* single mutants and two *xlg1-2 xlg3-2* double mutants lines (DM16 and DM34). As controls, hypersensitive (ctr1) and hyposensitive (ctr2) lines were used, which correspond to a *serk1-1serk3-1* loss of function line and a *serk1-1serk3-2* gain of function, respectively (Hohmann et al., 2018).

Significant differences could be observed for the *xlg3-2* mutant compared to wild-type, while the *xlg1-2* and *spx1-1* mutant were similar to wild-type. The two double mutant lines (DM16 and DM34) showed the same tendency as *xlg3-2*, suggesting that the hypersensitive phenotype is due to the *XLG3* mutation (Table 7 and Figure 11).

Comparaisons	Ratio-of-ratios	LowerCI	UpperCI
xlg3/WT	0,8736613	0,8178546	0,9332759
xlg1/WT	1,0561184	0,9894037	1,1273317
spx1/WT	1,0836141	1,0187678	1,1525881
DM34/WT	0,9091783	0,852759	0,9693303
M16/WT	0,9032451	0,845934	0,964439
ctr2/WT	1,6184767	1,520968	1,7222367
ctr1/WT	0,6821381	0,6423553	0,7243847

Table 7. Quantification of the data from Figure 11. The hypocotyl length was analyzed by a mixed effects model for the ratio of the transgenic lines vs. wild type (see methods). CI, confidence interval.

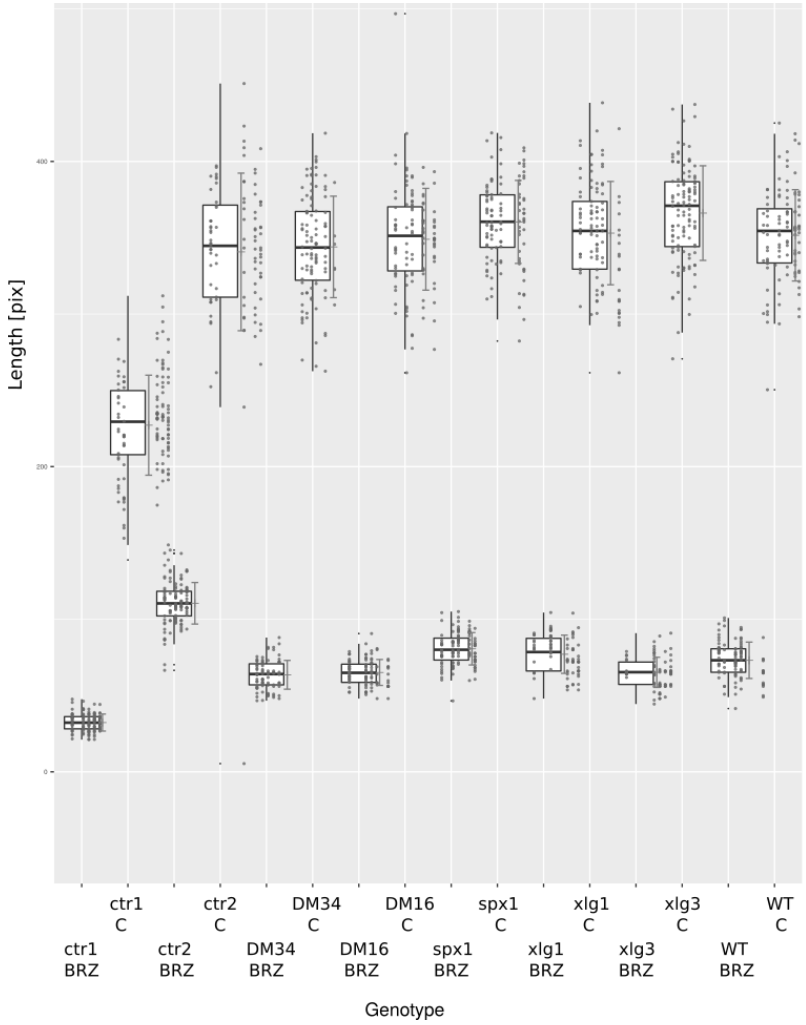

Fig 11. Box-plots representation of the hypocotyl growth assay, from seedlings grown for 5 d in the dark in the absence (C) or presence (BRZ) of BRZ of treated and untreated wild-type and mutant lines. Raw data is represented as dots. Data were analyzed using the package multcomp (Hothorn et al., 2008).

6. DISCUSSION AND CONLUSIONS

Signaling pathways involve diverse protein interactions to provide specificity for distinct stimuli. During this study, different phenotypic and interaction assays were performed to better understand the role of XLGs proteins in plant signaling pathways.

When the germination availability of different *xlg* mutants were tested, any mutant showed any phenotype under different light and temperatures conditions. However, the *in vitro* growth conditions in this assay were highly different to the natural soil. Therefore, future approaches could test the germination rate under different medium plates conditions, such as variable sucrose and phosphate concentrations.

Under Pi sufficient conditions, plants usually capture more Pi and store it inside the vacuole (Sakano et al., 1995). SPX1, SPX2, PHR1 and PHL1 play a role in the Pi uptake, and one characteristic phenotype is that the total Pi content in double *spx1-1 spx2-1* and *phr1-2 phl1* mutant plants is different from the wild-type levels (Bustos et al, 2010, Puga et al. 2014, this study). In this study, the first approach to study whether the XLGs impact Pi uptake was the measurement of the total Pi content in shoots of different *xlg* single and double mutants. We showed that under Pi sufficient conditions, the single *xlg1-2* and *xlg3-2* mutants have a decrease in Pi accumulation compared to the wild-type, and this difference was more pronounced in the two *xlg1-2 xlg3-2* double mutant lines analyzed (DM16 and DM34). Thus, these results suggest that both XLG1 and XLG3 play a role in Pi homeostasis. It is also reported here that the total Pi content can be more variable depending on the development stage of the plant. Therefore, to confirm the phenotype shown here more assays should be carried out, and the results should be reproducible.

The *xlg2-1 xlg3-1* double mutant and the *xlg1-1 xlg2-1 xlg3-1* triple mutant showed longer primary roots as wild-type plants when grown in darkness (Ding et al., 2008). Here we reported that only under Pi starvation conditions, *xlg1-2 xlg3-2* double mutants had an increased in primary root length, while the *phr1-2phl1* seedlings have decreased roots. The single *xlg* mutants do not show such difference, suggesting that both XLG1 and XLG3 are responsible for the phenotype observed in the double mutant lines. The *spx1-1spx2-1* mutant shows a tendency to form shorter primary roots, but the phenotype in this line is not as remarkable. To further study this phenotype, the growth of each genotype under different phosphate conditions could be analyzed.

Under Pi limiting conditions, the expression of PSI genes mediate different plant responses to facilitate Pi acquisition and remobilization (e.g., changes in the root system architecture). In several mutants of Pi signalling genes, e.g. *spx1-1spx2-1* and *phr1-2phl1*, the expression of PSI genes is perturbated (Puga et al. 2014, Bustos et al. 2010, this study). Here we observed that under Pi limiting conditions, the induction of PSI genes is enhanced in the tested *xlg* mutants compared to the wild-type, suggesting a direct or at least indirect connection between XLG signalling and Pi homeostasis. However, in the present study, the variation of the data was high, making it impossible to draw justified conclusions. Therefore, to support this conclusion, the same results should be obtained in a proper repetition of the experiment. In addition, it would

be interesting to include the analysis of PSI gene expression under Pi sufficient conditions as it has already been reported that *spx1-1spx2-1* and *phr1-2phl1* mutants also behave differently to the wild-type under these conditions.

The goal of looking for minimal fragments of AtXLG proteins that still interacting with AtSPX proteins would allow the use of these constructs in biochemical and crystallization experiments. Once the minimal fragments have been mapped down, it would be interesting to check whether these interactions are also PP-InsPs dependent. Thus, 2 new ΔVip1 lines should be produced, one expressing AtSPX1 and AtXLG1mini and a second one expressing AtSPX-MFS1 and AtXLG3supermini.

For the study of the PP-InsPs depending interaction, only the influence of 1-$InsP_6$ and 1,5-$InsP_6$ has been studied. However, it would be interesting to further analyze and compare the results here reported with the role of others PP-InsPs molecules such as 5-$InsP_6$. For this aim, the same approach would be carried out by using ΔKcs1 yeast, in which the other enzyme involved in PP-InsPs synthesis is mutated (Figure 8). Additionally, another interesting assay could be reproduced using a double ΔKcs1 and ΔVip1 yeast line, in which no PP-InsPs would be present.

It is important to take into account that the conclusions reported are based on the growth rate of different yeast lines, since the same number of cells were plated. However, the level of expression could be variable. Thus, to confirm that the level of growth is proportional to the interaction, a protein extraction and quantification via immunoblot should be executed. That would allow not only to check the presence of interaction between different constructs but also to compare the level of interaction between them.

Brassinosteroids (BRs) are steroid plant hormones implicated in complex signaling pathways that respond to abiotic environmental stresses (Bajguz and Hayat, 2009), and BR transcriptional effectors play key roles in plant adaptation to phosphate deficient environments. Phosphate deprivation reduces the expression levels of BR biosynthesis genes and contribute to the root response, whereas high BR levels block root response (Singh et al., 2014). Here we report that XLG3 may play a role in BR signaling, since the *xlg3-2* mutant line is hypersensitivity to BRZ. This phenotype is characteristic for the *serk1-1 serk3-1* line, which lacks the functional BR co-receptors SERK1 and SERK3 (Hohmann et al., 2018).

All the results showed in this project support a putative role of XLGs proteins, together with SPX proteins, in the maintenance of Pi homeostasis in *Arabidopsis thaliana*. In addition, these XLG proteins may also be involved in different signaling pathways, such as hormone responses. However, further studies should be carried out to define these proteins work.

7. REFERENCES

1. Binder A., Lambert J., Morbitzer R., Popp C., Ott T., Lahaye T. & Parniske M. (2014). A modular plasmid assembly kit for multigene expression, gene silencing and silencing rescue in plants. *PLoS ONE 9*: e88218.

2. Bajguz, A., & Hayat, S. (2009). Effects of brassinosteroids on the plant responses to environmental stresses. *Plant Physiol. Biochem*. 47, 1–8.

3. Bustos R., Castrillo G., Linhares F., Puga, M.I., Rubio V., Pérez-Pérez J., Solano R., Leyva A. & Paz-Ares, J. (2010) A central regulatory system largely controls transcriptional activation and repression responses to phosphate starvation in Arabidopsis. *PLoS Genet*. 6, e1001102.

4. Duan, K., Yi, K.K., Dang, L., Huang, H.J., Wu, W., & Wu, P. (2008). Characterization of a sub-family of Arabidopsis genes with the SPX domain reveals their diverse functions in plant tolerance to phosphorus starvation. *Plant J*. 54, 965–975.

5. Ding L., Pandey S. & Assmann S.M. (2008). Arabidopsis extra-large G proteins (XLGs) regulate root morphogenesis. *Plant J*, 53, 248-263.

6. Ezawa T. & Saito K. (2018). How do arbuscular mycorrhizal fungi handle phosphate? New insight into fine-tuning of phosphate metabolism. *New Phytologist*.

7. Heo JB., Sung S. & Assmann SM. (2012) Ca2+-dependent GTPase, extra-large G protein 2 (XLG2), promotes activation of DNA-binding protein related to vernalization 1 (RTV1), leading to activation of floral integrator genes and early flowering in Arabidopsis. *J Biol Chem* 287: 8242–8253.

8. Hohmann U., Nicolet J., Moretti A., Ludwig A., Hothorn LA. & Michael Hothorn (2018). The SERK3 elongated allele defines a role for BIR ectodomains in brassinosteroid signalling. *Nature Plants* 4, 345–351.

9. Hothorn T, Bretz F. &Westfall P (2008) Simultaneous inference in general parametric models. *Biom J* 50(3):346–363.

10. Jung J.Y., Ried M.K., Hothorn M. & Poirier Y. (2018). Control of plant phosphate homeostasis by inositol pyrophosphates and the SPX domain. *Current Opinion Biotechnol*, 49:156-162.

11. Lee YR. & Assmann SM. (1999) *Arabidopsis thaliana* 'extra-large GTP-binding protein' (AtXLG1): a new class of G-protein. *Plant Mol Biol* 40: 55–64.

12. Lopez-Bucio J., Cruz-Ramirez A. & Herrera-Estrella L. (2003) The role of nutrient availability in regulating root architecture *Current Opinion in Plant Biology* 6, 280–287.

13. Maruta N., Trusov Y., Brenya E., Parekh U. & Botella J. R. (2015). Membrane-localized extra-large G proteins and Gbg of the heterotrimeric G proteins form functional complexes engaged in plant immunity in Arabidopsis. *Plant Physiol*. 167, 1004–1016.

14. Marschner H. Mineral nutrition of higher plants. 2nd edn. London: Academic Press; 1995.

15. Pandey S., Monshausen GB., Ding L. & Assmann SM. (2008) Regulation of root-wave response by extra large and conventional G proteins in *Arabidopsis thaliana*. *Plant J* 55: 311–322.

16. Péret B., Clément M., Nussaume L. & Desnos T. *(2011)*. Root developmental adaptation to phosphate starvation: better safe than sorry. *Trends in Plant Science* 16, 442–450.

17. Poirier Y. & Bucher M. (2002) Phosphate transport and homeostasis in Arabidopsis. In The Arabidopsis Book, *C.R. Somerville and E.M. Meyerowitz, eds (Rockville, MD: American Society of Plant Biologists).*

18. Puga MI., Mateos I., Charukesi R., Wang Z., Franco-Zorrilla JM., de Lorenzo L., Irigoyen ML., Masiero S., Bustos R., Rodriguez J., Leyva A., Rubio V., Sommer H. & Paz-Ares J. (2014)SPX1 is a phosphate-dependent inhibitor of Phosphate Starvation Response 1 in *Arabidopsis*. *Proceedings of the National Academy of Sciences of USA*.;111:14947–14952.

19. Qi WJ., Manfield IW., Muench SP. & Baker A. (2017) AtSPX1 affects the AtPHR1–DNA-binding equilibrium by binding monomeric AtPHR1 in solution. *Biochem. J. 474, 3675–3687.*

20. Rubio V., Linhares F., Solano R., Martin AC., Iglesias J., Leyva A. & Paz-Ares J. (2001) A conserved MYB transcription factor involved in phosphate starvation signaling both in vascular plants and in unicellular algae. *Genes Dev*. 15, 2122–2133.

21. Sakano K., Yazaki Y., Okihara K., Mimurata T. & Kiyota S (1995) *Plant Physiol.* 108, 295-302.

22. Schindelin J., Arganda-Carreras I., Frise E, Kaynig V., Longair M., Pietzsch T., Preibisch S., Rueden C., Saalfeld S., Schmid B., Tinevez JY., White DJ., Hartenstein V., Eliceiri K., Tomancak P. & Cardona A. (2012) Fiji: a open-source platform for biological-image analysis. *Nat Methods* 9(7):676-682.

23. Singh A., Fridman Y., Friedlander-Shami L., Tarkowska D., Strnad M., Savaldi-Goldstein S. (2014) Activity of the brassinosteroid transcription factors B RASSINOSTEROID INSENSITIVE1-ETHYL METHANESULFONATE-SUPPRESSOR1/BRASSINAZOLE RESISTANT2 blocks developmental reprogramming in response to low phosphate availability. *Plant Physiol* 166:678-688.

24. Secco D., Wang C., Arpat BA., Wang Z., Poirier Y., Tyerman SD., Wu .P, Shou H. & Whelan J. (2012). The emerging importance of the SPX domain-containing proteins in phosphate homeostasis. *New Phytol* 193(4):842-51.

25. Urano D., Chen J-G., Botella JR. & Jones AM (2013). Heterotrimeric G protein signalling in the plant kingdom. *Open Biol.* 3:120186.

26.Ullah H., Chen J. G., Young J. C., Im K. H., Sussman M. R. & Jones A. M. (2001). Modulation of cell proliferation by heterotrimeric G protein in Arabidopsis. *Science* 292, 2066–2069.

27. Wild R., Gerasimaite R., Jung J.Y., Truffault V., Pavlovic I., Schmidt A., Saiardi A., Jessen H.J., Poirier Y., Hothorn M. & Mayer A (2016). Control of eukaryotic phosphate homeostasis by inositol polyphosphate sensor domains. *Science*, 352(6288):986-90.

28. Zhu H., Li GJ., Ding L., Cui X., Berg H., Assmann SM. & Xia Y. (2009) Arabidopsis extra-large G-protein 2 (XLG2) interacts with the Gβ subunit of heterotrimeric G protein and functions in disease resistance. *Mol Plant* 2: 513–525.